# Supplementary Information

# Removing interference-based effects from the infrared transflectance spectra of thin films on metallic substrates: A fast and wave optics conform solution

Thomas G. Mayerhöfer[a,b,*], Susanne Pahlow[b], Uwe Hübner[a], Jürgen Popp [a b]

*a Leibniz Institute of Photonic Technology (IPHT), Albert-Einstein-Str. 9, D-07745 Jena, Germany*
*b Institute of Physical Chemistry and Abbe Center of Photonics, Friedrich Schiller University, Jena, D-07743, Helmholtzweg 4, Germany*
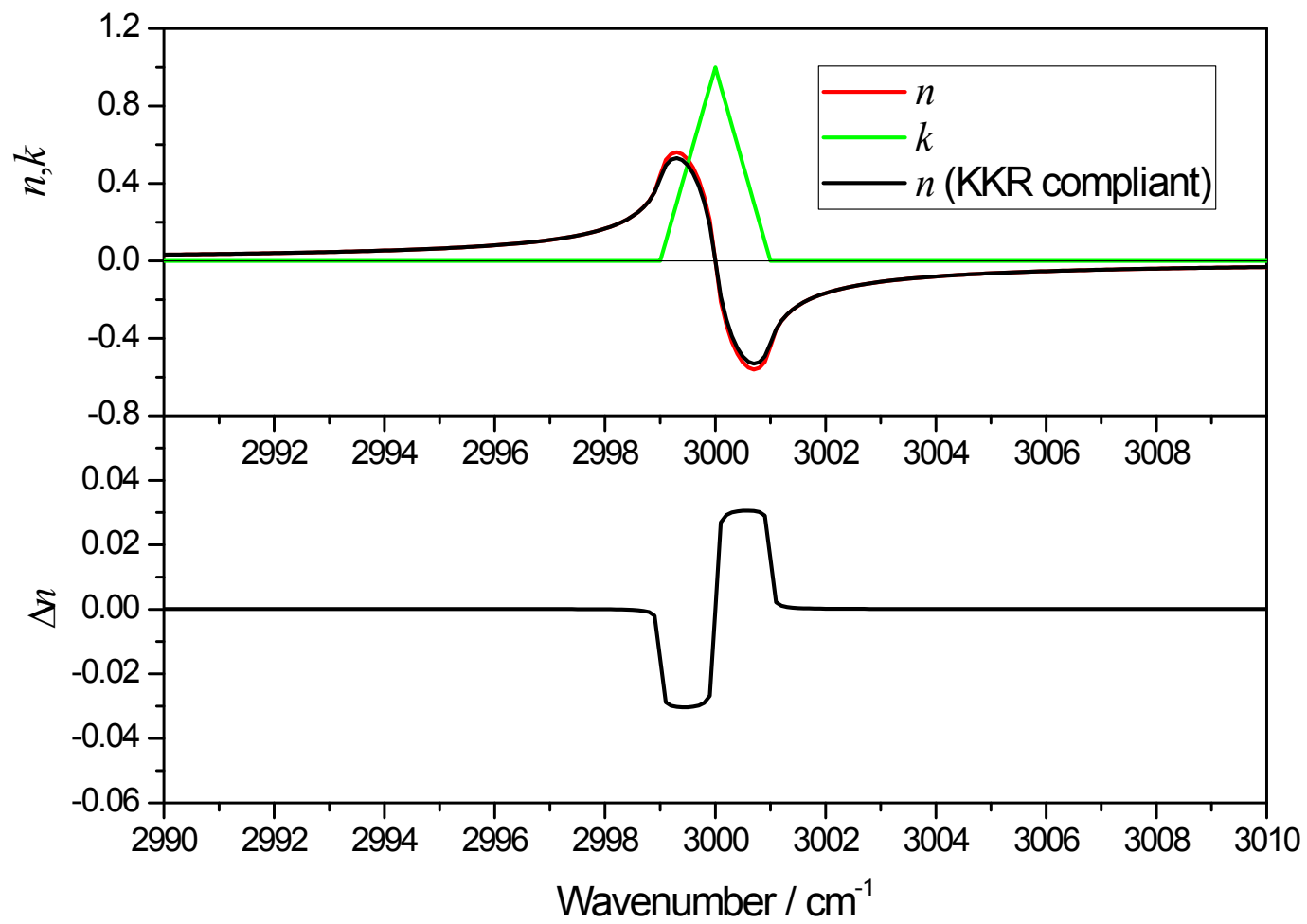
*Figure SI 1:* Triangular basis function and comparison between its real part calculated with eqn. (3) (black curve) and eqn. (5) (red curve).
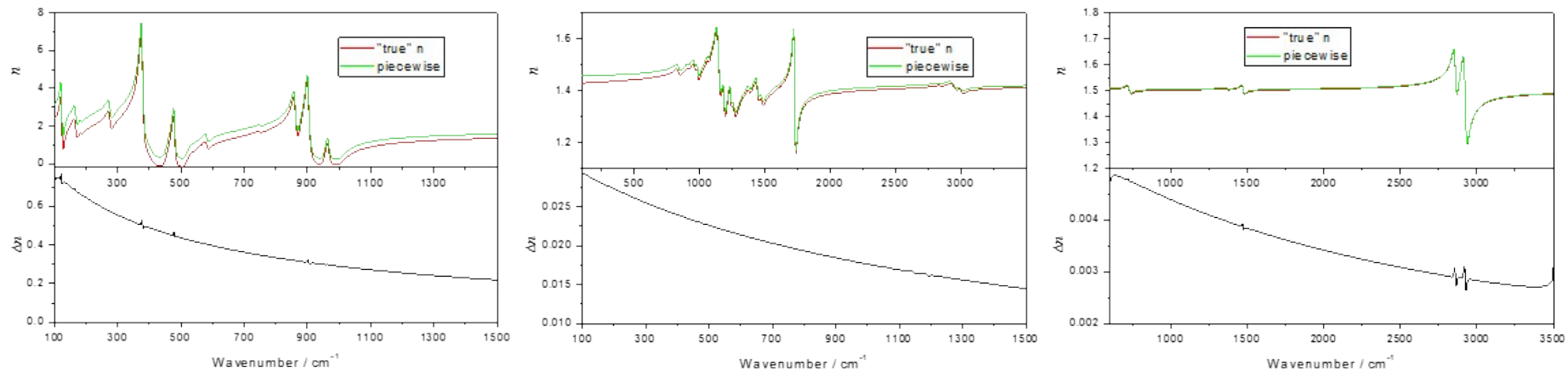
*Figure SI 2:* Comparison between the Kramers-Kronig compliant real parts calculated with eqn. (2) (red curves) and eqn. (5) (green curves) for fresnoite (*a*-cut, left graph), PMMA (center graph) and Polyethylene (right graph).

| # | 1 | 2 | 3 | 4 | 5 | 6 | 7 | 8 | 9 |
|---|---|---|---|---|---|---|---|---|---|
| S | 46.9 | 51.3 | 34.9 | 66.7 | 53.1 | 34.8 | 198.6 | 120.4 | 92.3 |
| $\gamma$ | 18.854 | 33.89 | 32.668 | 32.369 | 17.328 | 17.315 | 37.811 | 27.006 | 23.638 |
| $\tilde{\nu}$ | 750 | 838.4 | 913.2 | 960.1 | 985.2 | 1063.3 | 1145.1 | 1186.1 | 1236.3 |
| # | 10 | 11 | 12 | 13 | 14 | 15 | 16 | 17 | |
| S | 100.5 | 57 | 106.3 | 72.8 | 201 | 34.9 | 123.6 | 74.4 | |
| $\gamma$ | 34.071 | 28.913 | 30.655 | 28.471 | 17.57 | 32.328 | 62.379 | 34.947 | |
| $\tilde{\nu}$ | 1263 | 1378.7 | 1441.8 | 1475.8 | 1727 | 2843 | 2946.4 | 3002.5 | |
| $\varepsilon_\infty$ | 2.034 | | | | | | | | |

| Parameter [units] | |
|---|---|
| $\lambda_p$ [nm] | 143 |
| $\gamma_p$ [nm] | 14500 |
| $A_1$ | 1.27 |
| $\phi_1$ [rad] | -π/4 |
| $\lambda_1$ [nm] | 470 |
| $\gamma_1$ [nm] | 1900 |
| $\phi_1$ [rad] | -π/4 |
| $\lambda_1$ [nm] | 325 |
| $\gamma_1$ [nm] | 1060 |
| $\varepsilon_\infty$ | 1.54 |

The values of *Table SI 2* have to placed into the following equation which is an extension of eqn. (2,II) taking into account the interband excitation of gold:

$$\varepsilon = \varepsilon_\infty - \frac{\tilde{\nu}_p^2}{\tilde{\nu}^2 + i\tilde{\nu}\tilde{\nu}_\gamma} + \sum_{j=1}^{2} A_j \left[ \frac{e^{i\phi_j}}{\tilde{\nu}_j - \tilde{\nu} - i\tilde{\nu}_{\gamma_j}} + \frac{e^{-i\phi_j}}{\tilde{\nu}_j + \tilde{\nu} + i\tilde{\nu}_{\gamma_j}} \right]$$

$A_j$ : dimensionless critical point amplitudes

$\tilde{\nu}_j$ : interband transition wavenumber

$\gamma_j$ : transition damping constants

$\phi_j$ : phase

*Table SI 3:* Values of $n_{\infty,calc}$ and $d_{calc}$ as obtained by the fitting procedure the results of which are shown in Fig. SI 6 (assumption: angles of incidence range from 10 to 54°, s-polarization) as well as the time necessary for the evaluation.

| $d$/nm | $n_{\infty,calc}$ | $d_{calc}$/nm | $t$/s |
|--------|-------------------|---------------|-------|
| 500 | 1.44 | 490 | 3.07 |
| 600 | 1.45 | 581 | 3.87 |
| 700 | 1.52 | 646 | 5.72 |
| 800 | 1.34 | 883 | 7.42 |
| 900 | 1.37 | 956 | 6.89 |
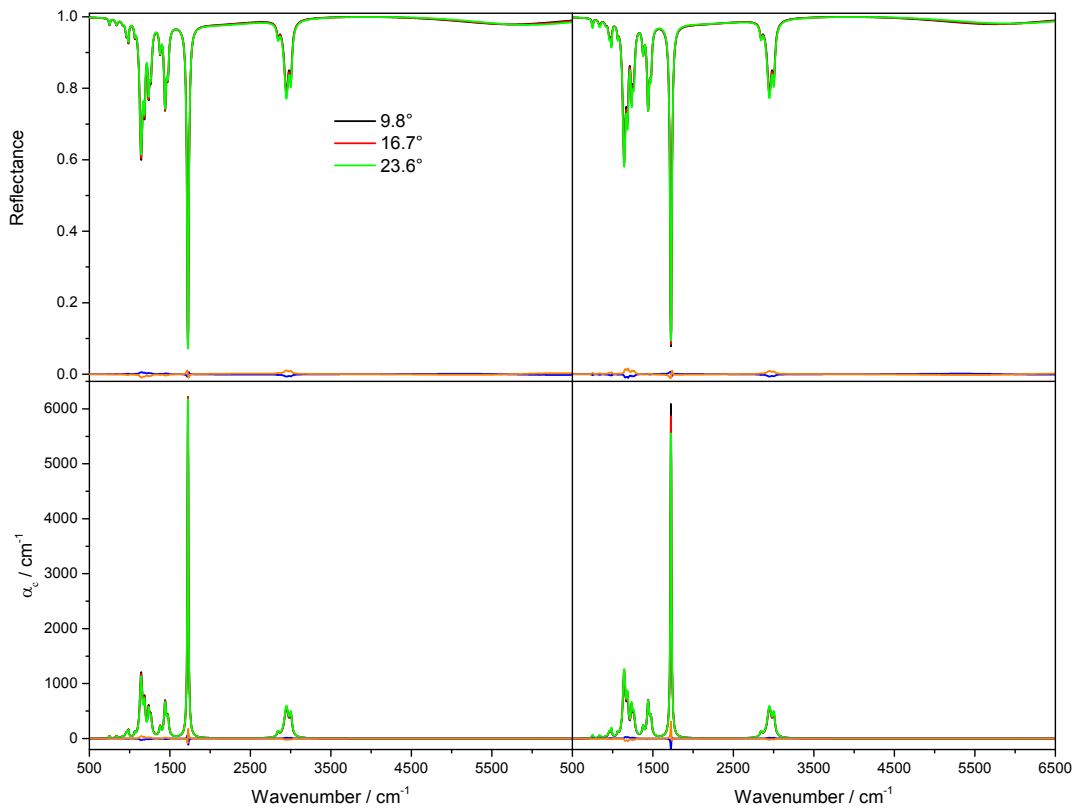
*Figure SI 3:* Spectra of a 900 nm thick PMMA layer on gold for different angles of incidence α (black: α = 9.8°, red: α = 16.7°, green: α = 23.6 °). The blue lines illustrates the difference between the red and the black spectra and the orange line the differences between the red and the green spectra. The left panels show s-polarized reflectance (upper panel) and s-polarized absorption coefficient (lower panel), whereas the p-polarized reflectance and absorption coefficient are shown in the right panels. A magnification for the blue and orange difference spectra is shown in Fig. SI 4.
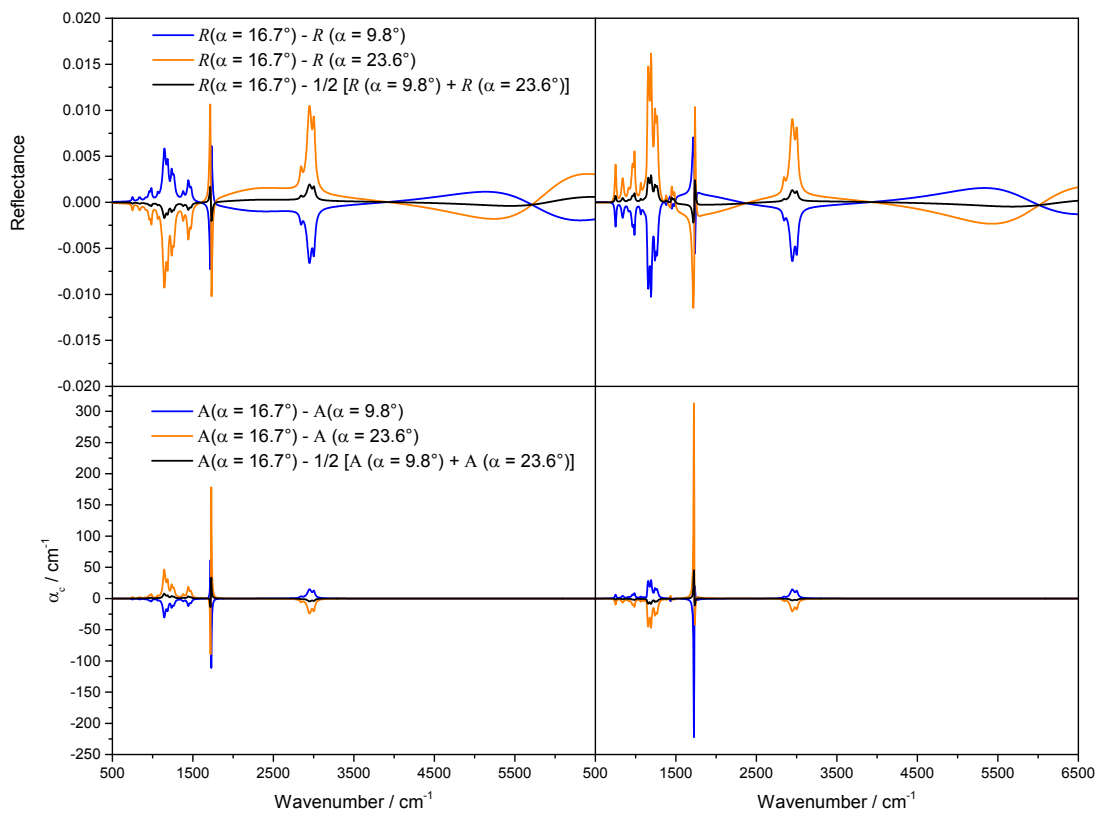
*Figure SI 4:* Difference Spectra of a 900 nm thick PMMA layer on gold for different angles of incidence $\alpha$ (blue: reflectance or absorbance for $\alpha = 16.7°$ – reflectance or absorption coefficient for $\alpha = 9.8°$, orange: reflectance or absorption coefficient for $\alpha = 16.7°$ – reflectance or absorption coefficient for $\alpha = 23.6$ °). The black lines illustrates the difference between the reflectance or absorption coefficient for $\alpha = 16.7°$ – the averaged reflectance or absorbance for $\alpha = 9.8°$ and $\alpha = 23.6°$. The left panels show s-polarized reflectance (upper panel) and s-polarized absorption coefficient (lower panel), whereas the p-polarized reflectance and absorption coefficient are shown in the right panels.
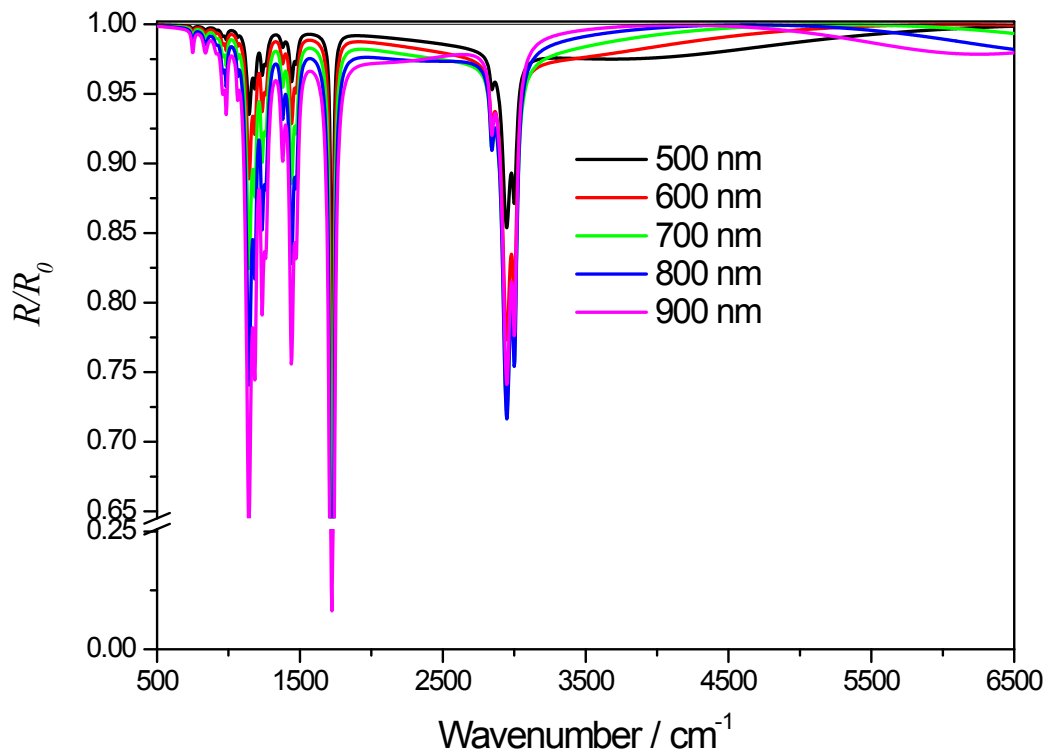
*Figure SI 5:* Synthetic transflection spectra of PMMA layers on gold with thicknesses ranging from 500 to 900 nm assuming an incidence angle range between 10 and 54° and s-polarization.
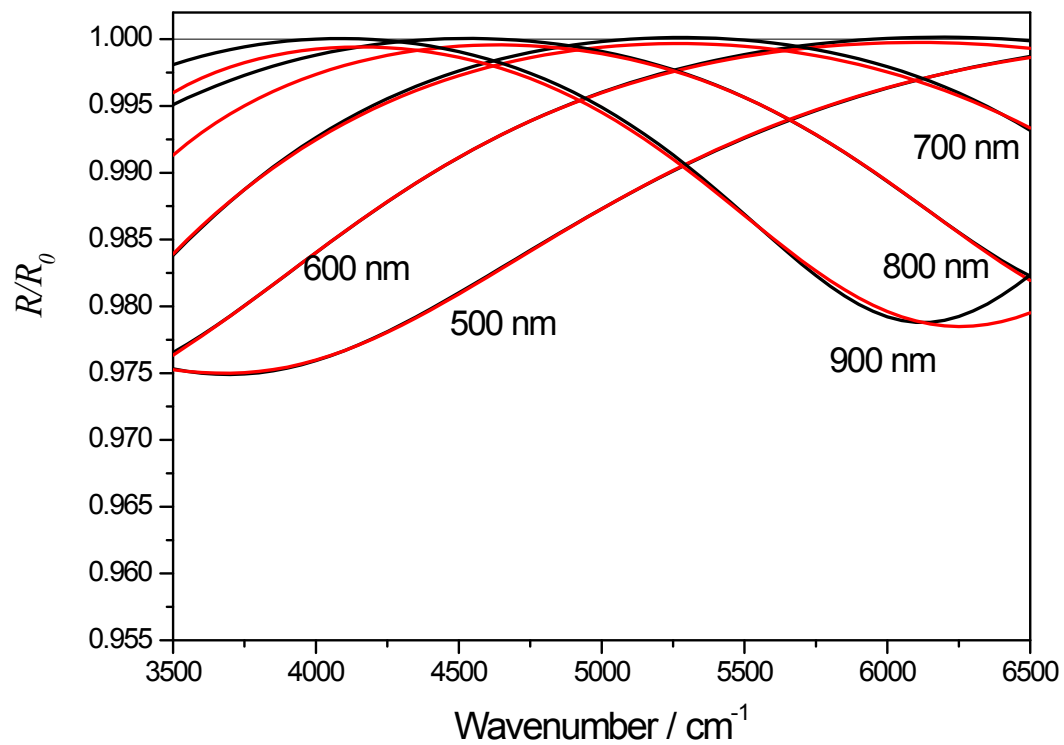
*Figure SI 6:* Fit of the synthetic transflection spectra of PMMA layers on gold assuming a constant and real refractive index $n_\infty$ (black curves) and comparison with the synthetic transflection spectra (in red, incidence angles range between 10 and 54°, and s-polarization is assumed). Cf. Table SI 3.
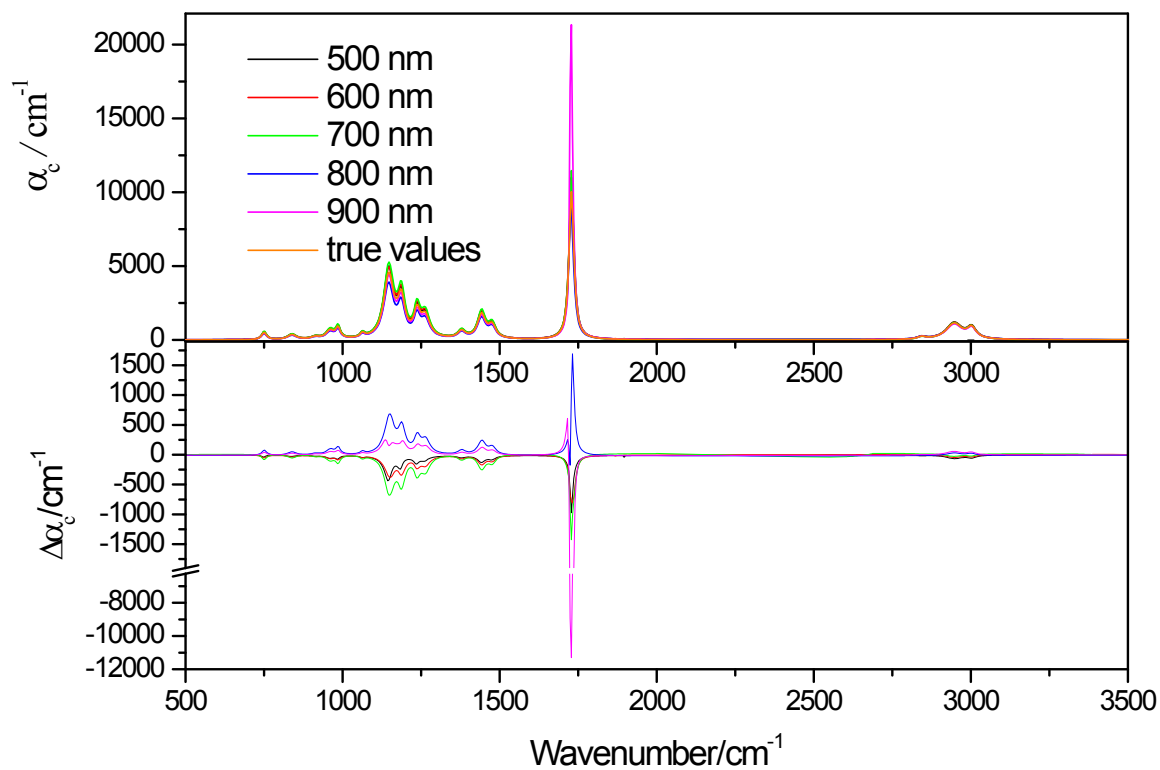
9

*Figure SI 7:* Absorption coefficient spectra of the PMMA layers on gold after application of the correction scheme and comparison with the true absorption coefficient spectrum assuming an incidence angle range between 10 and 54° and s-polarization.
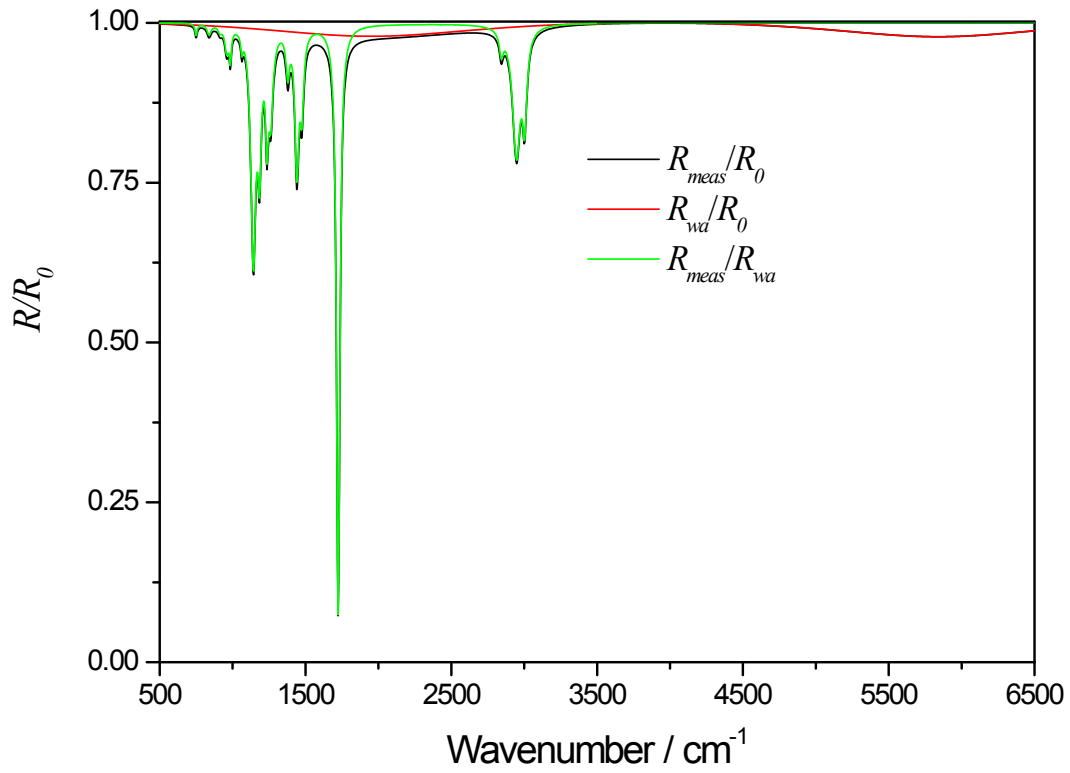
*Figure SI 8:* Removal of fringes by dividing the measured transflection spectrum (in this figure, not a measured, but a synthetic PMMA spectrum with $d = 900$ nm) by a spectrum of an imaginary layer with the same $d$ and $n_\infty$, but without absorption. Black curve: Measured reflectance spectrum $R_{meas}$ divided by the reflectance of pure gold $R_0$; red curve: Calculated spectrum assuming a layer with the same $d$ and $n_\infty$, but without absorption $R_{wa}$ divided by the reflectance of pure gold; green curve: $R_{meas}/R_{wa}$
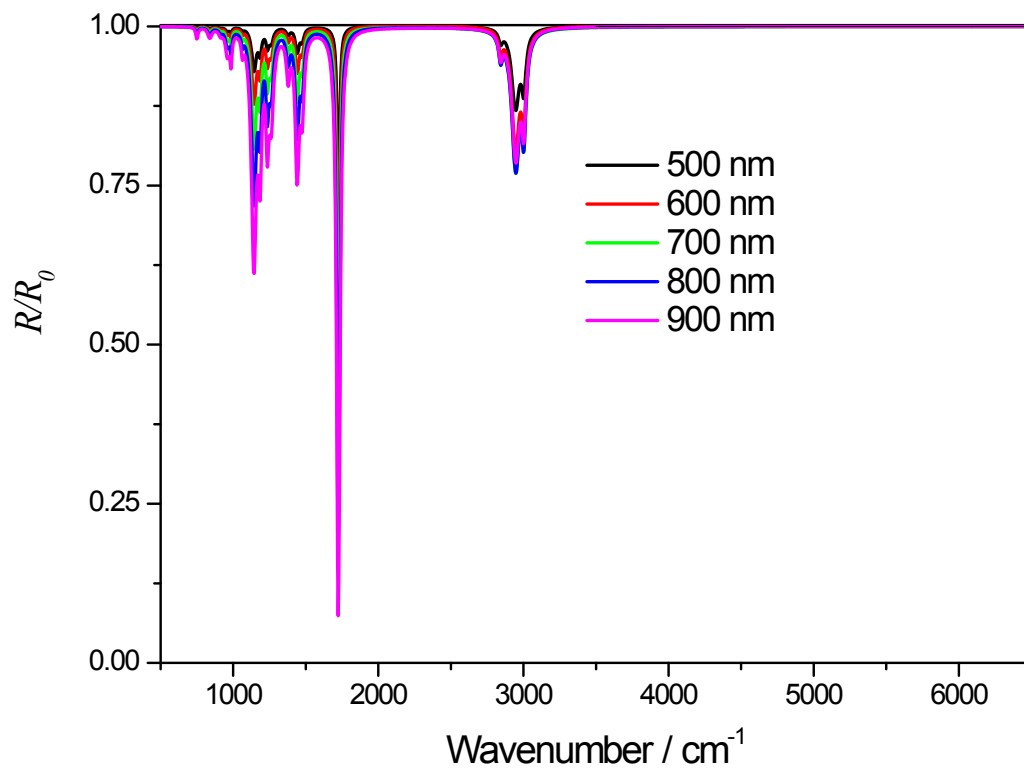
*Figure SI 9:* Baseline-corrected synthetic spectra $R_{meas}/R_{wa}$ of PMMA on gold.
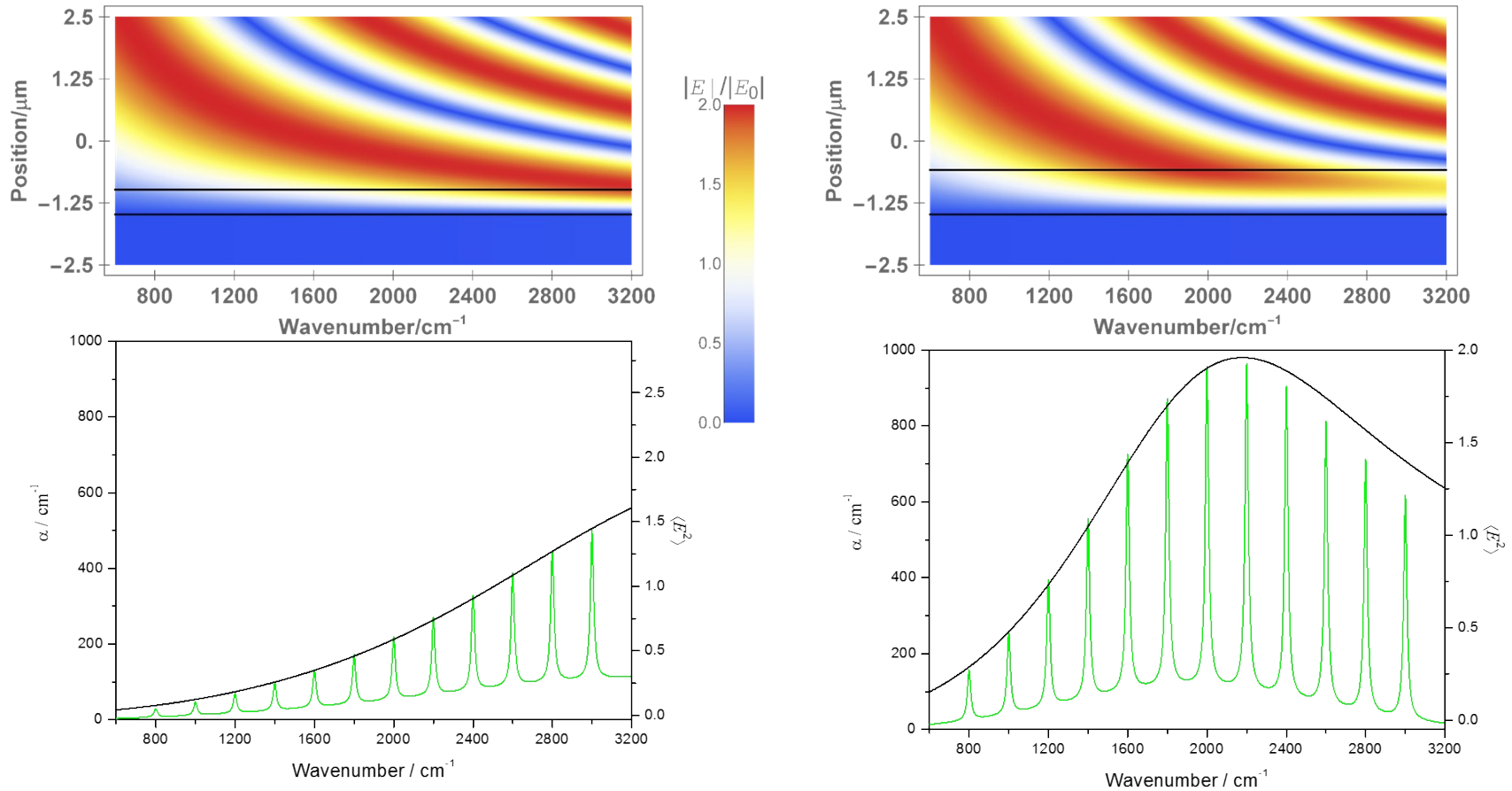
*Figure SI 10:* Upper panels: Electric field distribution maps for two layers of non-absorbing materials on gold. The gold layer extends from -2.5 to -1.5 μm. The non-absorbing layer is 500 nm thick in the left upper panel and 900 nm thick in the right upper panel (framed by black lines). Above the non-absorbing layer is the incidence medium. Lower panels: Apparent absorption coefficient spectra, if the layered medium would be absorbing with absorption bands of equal intensity in the true absorption coefficient spectra every 200 cm$^{-1}$. The different absorption strengths are a consequence of the electric field intensities, i.e. the electric field squared, inside the layer, the averages of which are given by the black lines (note that, since the Electric field distribution maps are for non-absorbing layers, the average electric field intensity of these layers is only approximately the contour for the bands).
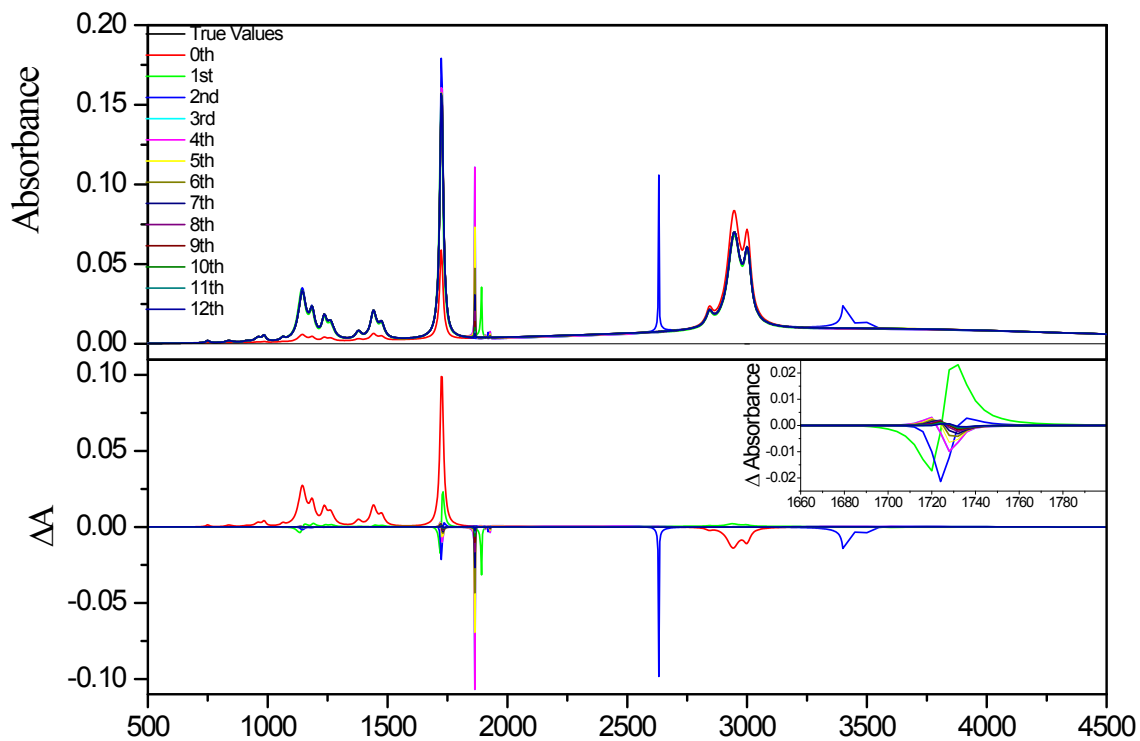
13

*Figure SI 11:* Progress of the iteration is exemplified for the 500 nm thick PMMA layer on gold. The first correction scheme according to eqn. (9) is used until the 4th iteration (which is already converged and identical to the 3rd iteration). Afterwards continuation with the 2nd convergence scheme following eqn. (10) until convergence is reached again (the dispersion analysis based 3rd correction scheme was not used in this case).
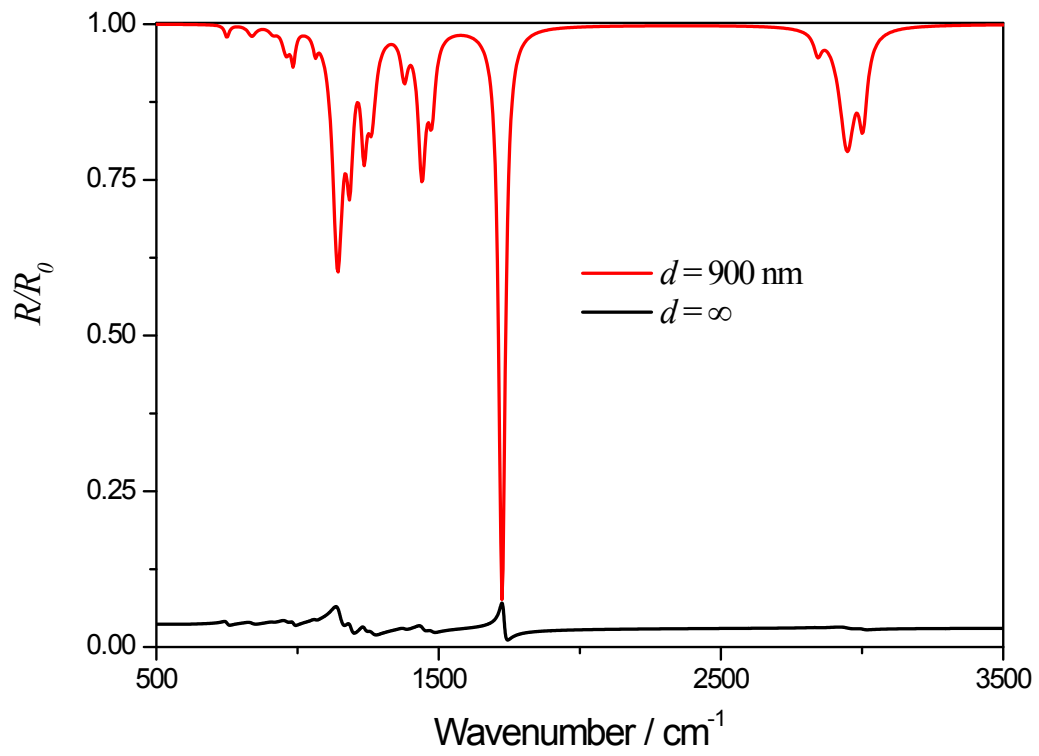
*Figure SI 12:* Comparison of the reflectance spectrum of a 900 nm thick PMMA layer on gold with that of an indefinitely thick PMMA layer.
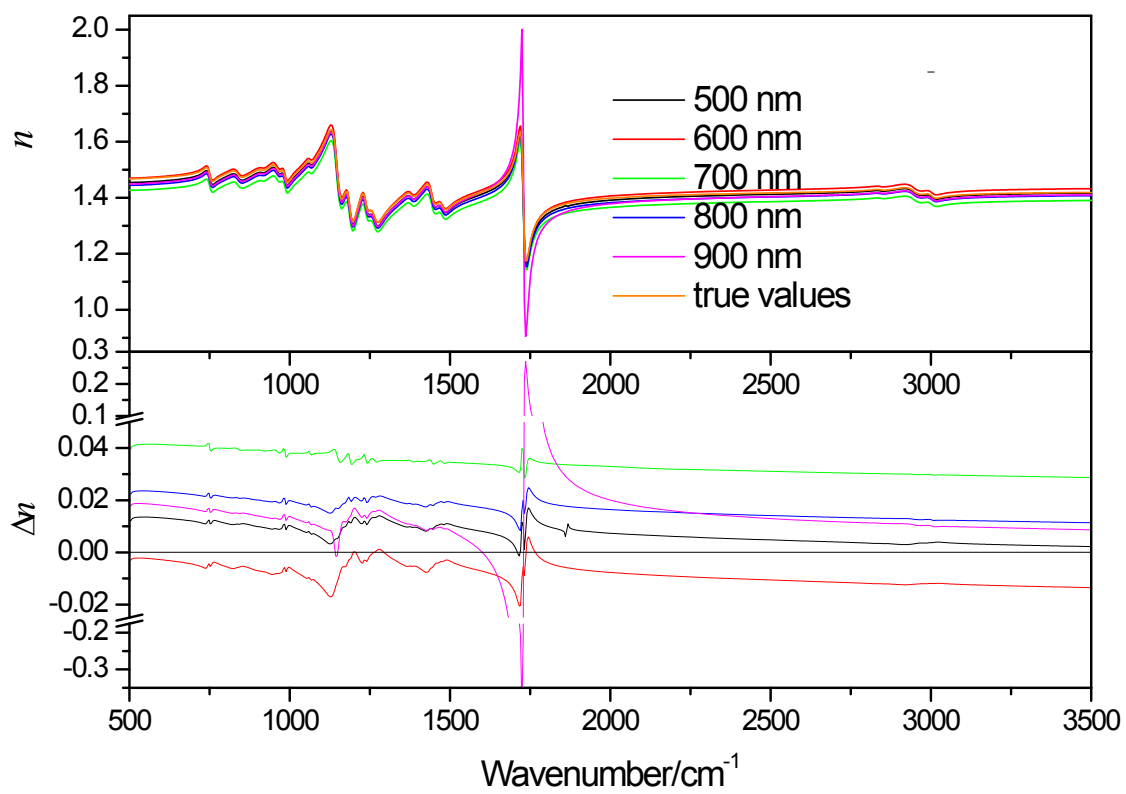
*Figure SI 13:* Comparison of the real part of the index of refraction function gained by the poor man's Kramers Kronig analysis with the true values.
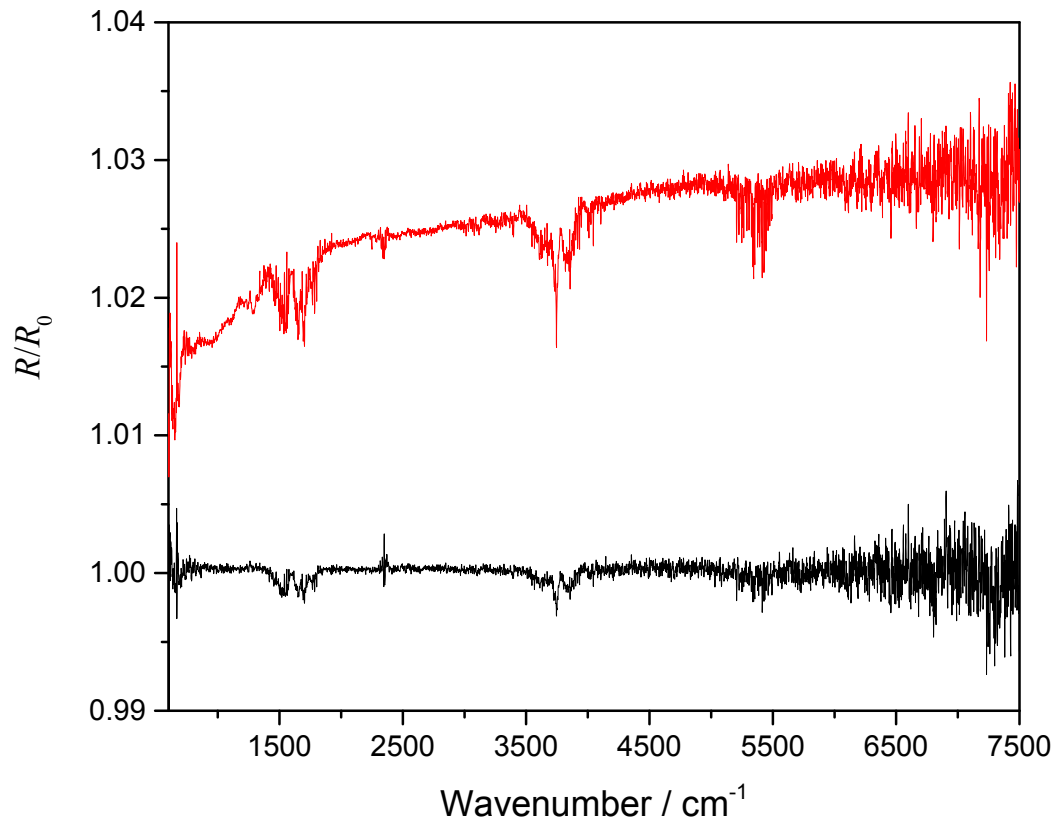
*Figure SI 14:* Comparison of the gold reference spectrum before the measurement of the first sample (black line) and after the last sample (red sample), which was the sample with a PMMA thickness of 580 nm.
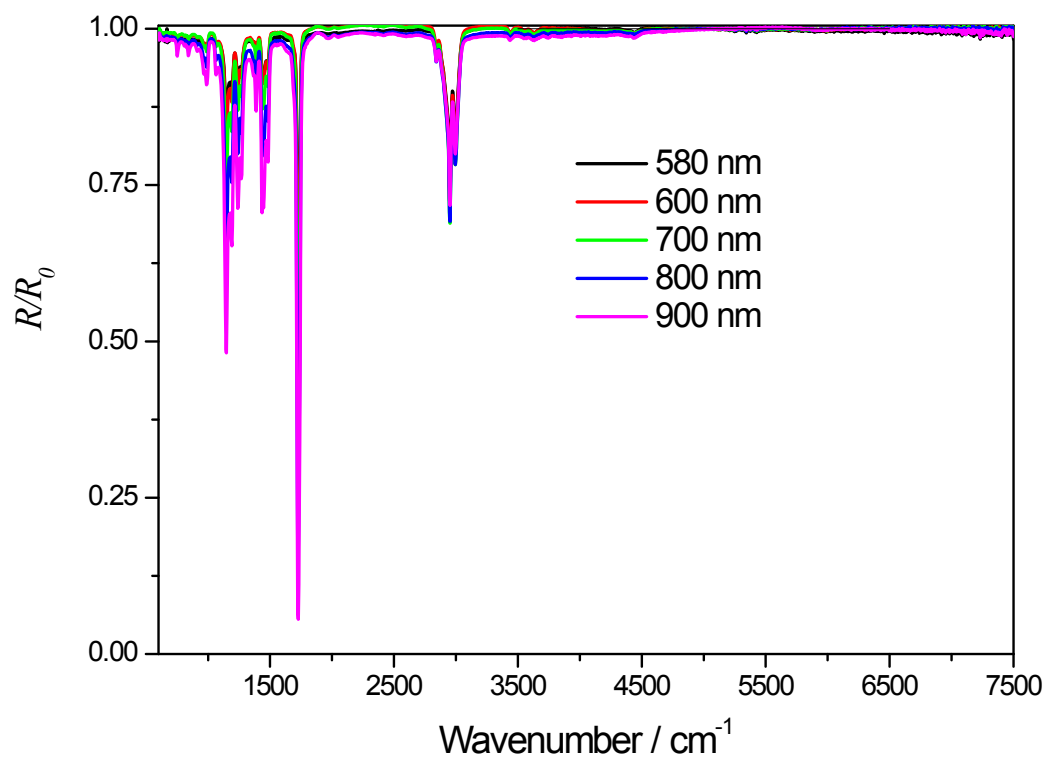
*Figure SI 15:* Baseline-corrected experimental spectra $R_{meas}/R_{wa}$ of PMMA on gold.
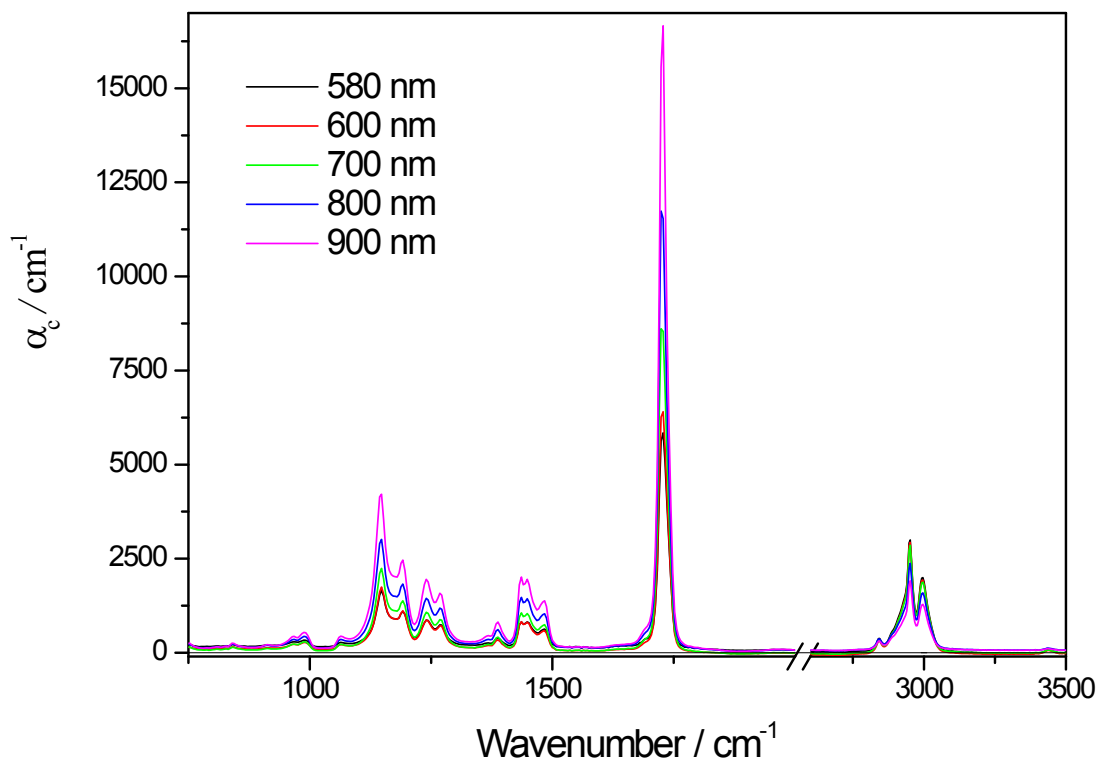
*Figure SI 16:* Apparent absorption coefficient spectra of the PMMA layers on gold calculated from the experimental spectra. For decreasing thickness, the region of maximum enhancement shifts from about 2000 cm$^{-1}$ to 3000 cm$^{-1}$, cf. Fig. SI 5.
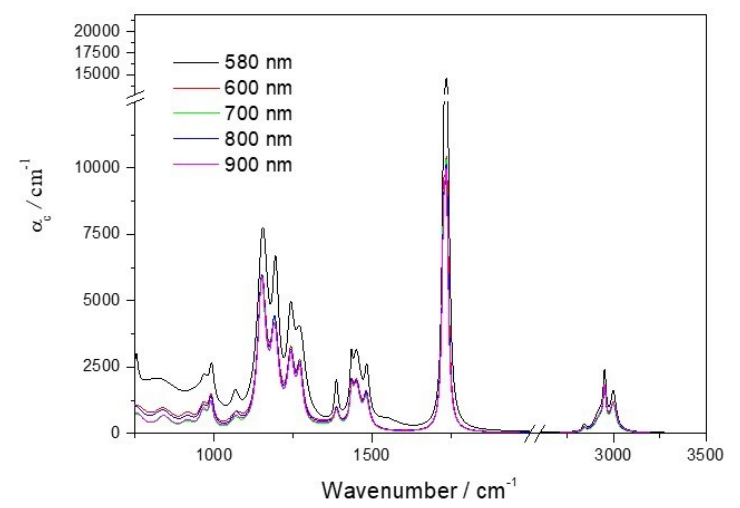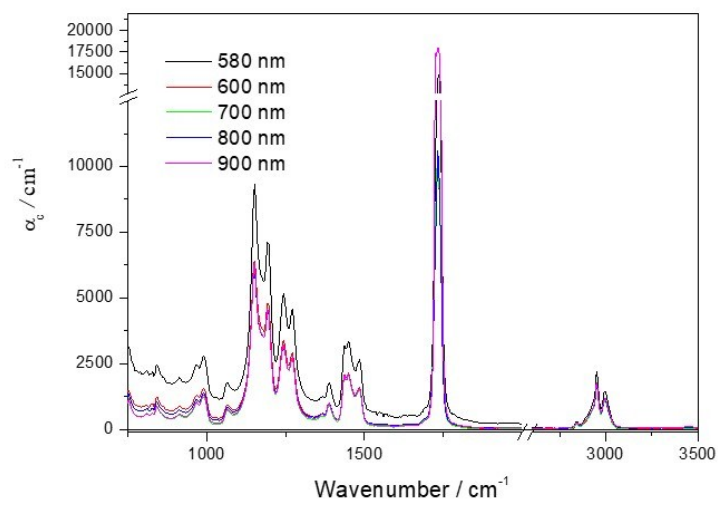
*Figure SI 17:* True absorption coefficient of the experimental spectra determined by the new formalism (left panel) and comparison with the results from dispersion analysis (right panel).

# REFERENCES

[1] R.T. Graf, J.L. Koenig, H. Ishida, Optical Constant Determination of Thin Polymer Films in the Infrared, Appl. Spectrosc., 39 (1985) 405-408.
[2] P.B. Johnson, R.W. Christy, Optical Constants of the Noble Metals, Physical Review B, 6 (1972) 4370-4379.
[3] P.G. Etchegoin, E.C. Le Ru, M. Meyer, An analytic model for the optical properties of gold, J Chem Phys, 125 (2006) 164705.
[4] P.G. Etchegoin, E.C. Le Ru, M. Meyer, Erratum: "An analytic model for the optical properties of gold" [J. Chem. Phys. 125, 164705 (2006)], The Journal of Chemical Physics, 127 (2007) 189901.